

A guideline for the synthesis and heterogeneous integration of two-dimensional germanium-based material

Md Rakibul Alam Bhuyan¹ and Md Iftekharul Alam Shovon²

¹Department of Electrical & Electronic Engineering, Sylhet Engineering College, SUST, Sylhet, Bangladesh

²Department of Electrical & Electronics Engineering, Sonargaon University, Dhaka, Bangladesh

Corresponding Author: Md Rakibul Alam Bhuyan

ABSTRACT

In recent years, germanium (Ge) based 2D material has drawn significant attention for its remarkable atomic structure, analogous to other group IV elements such as graphene and silicene. This arrangement provides high carrier mobility and a large bandgap, creating promising candidates for electronic, thermoelectric, and optoelectronic devices. Unlike graphene, germanium and its 2D derivatives can be easily tuned by chemical functionalization, which has made an extraordinary achievement in catalysis and energy storage applications. This work summarizes the fabrication of free-standing (FS) germanene sheets on different metallic, semimetallic, and semiconductive substrates, as well as their properties (mechanical and electrical). Afterward, germanene's methyl and hydrogen-terminated (functionalized) formation processes are briefly illustrated and differentiated by the properties of different topotactical deintercalation approaches. Finally, this review concludes with an outlook on the progress and critical challenges of Ge-based 2D materials based on recent developments.

KEYWORDS;- 2D material, carrier mobility, catalysis, electronic property, energy storage, cancer treatment, germanene

Date of Submission: 05-04-2025

Date of acceptance: 15-04-2025

I. INTRODUCTION

The novel graphene 2D material is popular for its extraordinary properties because of the honeycomb structure with sp^2 hybridization. Therefore, the researcher has been interested in further analysis of other group IV elements, such as silicon (Si), germanium (Ge), and tin (Sn), which contain analogous electronic configurations to C, the atomic form of graphite or graphene oxide. However, the 2D materials silicene (Si) and germanene (Ge) are artificially made to synthesize buckled honeycomb lattices. This structure engenders excellent properties such as bandgap and strongly predicted spin-orbit gap (24 meV), indicating the ideal applicant to exhibit the quantum spin hall effect (QSHE) [1]. Germanene 2D sheet behaves as a topological insulator protecting the spin-polarized edge mode, which disappears the charge conductance and specific value of spin conductance [3], [4].

Moreover, the buckled structure significantly affects the high intrinsic carrier mobility (ICM) of germanene sheets that can achieve $\sim 6 \times 10^5 \text{ cm}^2 \text{V}^{-1} \text{s}^{-1}$, which induces a crucial factor in semiconductor materials [5],[6]. Ye et al. calculated the first principal methodology of the ICM in germanene using the Boltzmann transport equation with time relaxation time and reported a larger mobility than graphene [5]. In addition, the theoretical hypothesis observed that germanene acts like a massless Dirac fermion and minimizes the electron-phonon coupling strength. Considering the impressive electronic properties of germanene has a promising future in energy storage, biosensors, optical devices, and thermal nanodevices applications [7–9].

Germanene is mainly fabricated by epitaxial growth on different metallic substrates such as Ag (111) [10], Pt (111) [11], Al (111) [12–14], Cu (111) [15], and Au (111) [16]. Therefore, the properties and characteristics differ based on the substrate. Most interestingly, the mechanical properties exhibit in multiple directions because of Stone-Wales defects, vacancies, and grain boundaries (GBs) during the fabrication process [16]. The crack mechanism and strain analysis of germanene obtained by the density functional theory (DFT) impact a lot of electronic properties of the nanodevices [17]. Moreover, germanene is able to be chemically functionalized easily compared to other Xenon (2D material), and it is expected to be used as a prospective anode material in energy storage applications [8].

This article summarizes the synthesis method of Ge-based 2D material in different substrates using chemical functionalization with their remarkable electrical and mechanical properties, stability, and their potential application field. We first introduce the fabrication of germanene by epitaxial growth on different metallic and semiconductor substrates and a study with the help of a scanning tunneling microscope (STM) and low-energy electron diffraction. Secondly, the functionalized germanene is presented with the chemical deintercalation technique for both CaGe_2 and doped CaGe_2 to investigate their electronic and mechanical properties and their stability after formation. Most importantly atomic structure of the Ge sheet is also analyzed, which is critical for defect-free or high-quality nanomaterials. Overall, we demonstrate a systematic technical outline of Ge-based 2D material based on experimental, computational analysis, and real-world application.

II. SYNTHESIS OF GERMANENE

Synthesis of high-quality germanene 2D nanosheets refers to any fabrication technique contingent upon the specific application's desired shape, size, and efflorescence. In early 2000, germanene was first reported by Vogg et al. as GeH on the CaGe_2 films by the epitaxial growth of topochemical transformation, which exhibited optical photoluminescence in the near infrared [18]. Later, Bianco et al. observed high-stability multi-layered Ge sheets with the help of topochemical deintercalation of CaGe [19]. In recent years, numerous procedures mechanical exfoliation [19], chemical exfoliation [18], chemical synthesis [20], and epitaxial growth on different substrates [21], have been chiefly used to synthesize germanene. In addition, other techniques such as electrochemical [22], plasma-assisted [23], and liquid phase exfoliation [24] are summarized in Fig.1

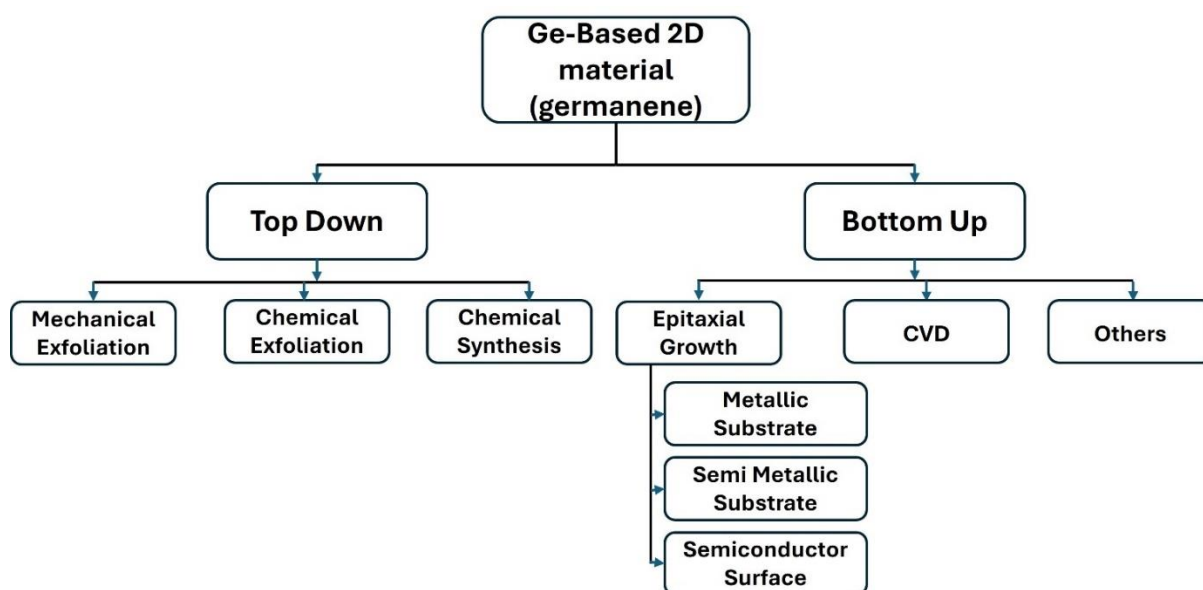


Fig. 1: Schematic synthesis flow chart of Ge-based 2D material.

To better understand the interatomic potential of single or multilayer synthesized germanene sheets was conducted using Density Functional Theory (DFT) [25]. Different polymorphs of germanene, flat, low-buckled, trigonal dumbbell, large honeycomb dumbbell, etc., were simulated by DFT to calculate the structural and mechanical properties of this 2D material, are shown in Fig. 2.

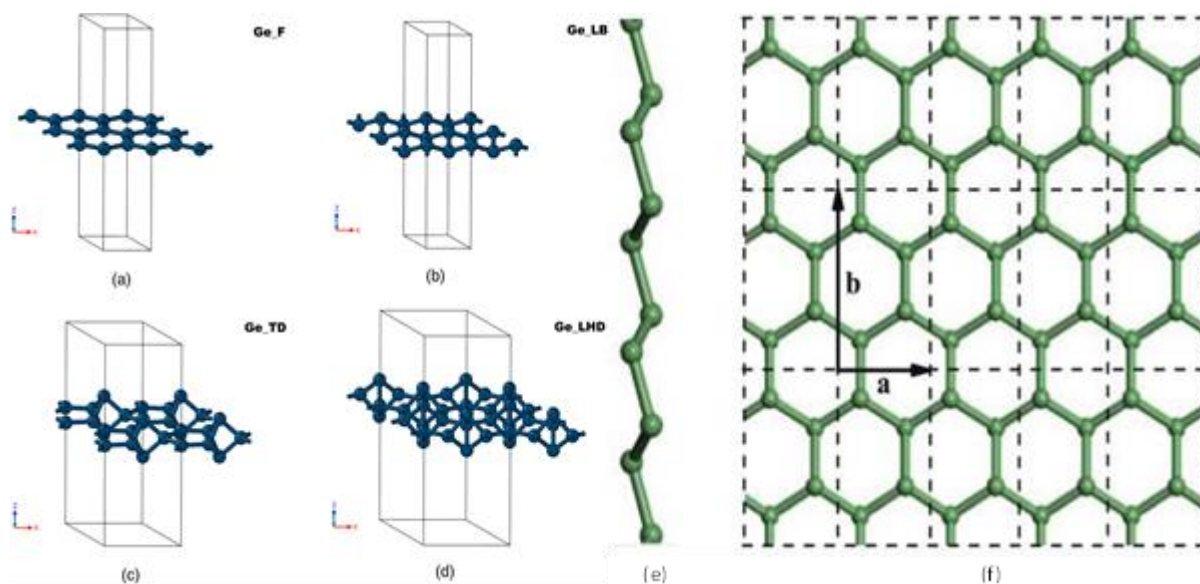


Fig. 2. Polymorphs of germanene: (a) flat (F), (b) low-buckled (LB), (c) trigonal dumbbell (TD), (d) large honeycomb dumbbell (LHD), permission of [25]. Also, a side(e) and a top (f) view of the honeycomb structure of germanene 2D sheet (a and b are the direction of dilation) from the permission of [5].

2.1 Top Down

Similar to other 2D materials, top-down techniques are popular to generate high-purity 2D Ge sheets in a large-scale format. Mainly, Top-down nanofabrication produces ultrathin nanosheets using either a physical or chemical technique. Chemical approaches of the top-down method avoid germanene and directly fabricate germanene when the Ge atom is saturated and has increased stability [26]. This procedure was followed earlier by Wallbaum in 1944 [27] and Vogt et al. in 2000 [28]. In 2013, the germanene drew significant attention when Goldberger and co-workers revealed the benefits of topochemical deintercalation of the Zintl phase, CaGe_2 , in concentrated acid, removing the Ca^{2+} interlayers to yield fully hydrogenated free-standing germanene layers [19]. Later, further advancement minimizes the multiple fabrication steps to a single step (methyl-terminated germanene, Ge-CH_3), obtaining high-quality covalent functionalized germanene [29]. Fig. 3 illustrates the exfoliation of topotactical deintercalation of Zintl phase to produce single or multilayers of germanenes or functionalized germanenes.

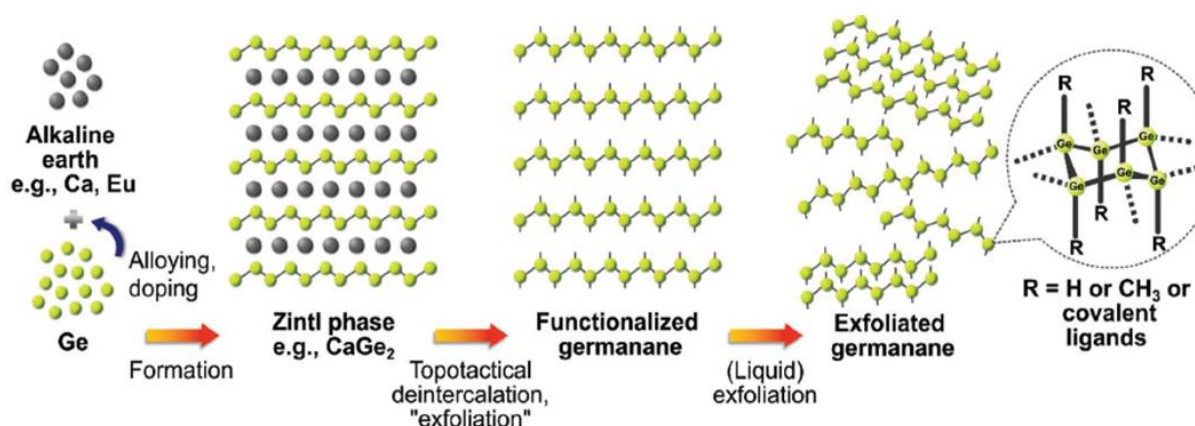


Fig 3. Typical route for the formation of (functionalized) germanenes. i) Synthesis of Zintl phase. ii) Topotactical deintercalation or “exfoliation” of Zintl phase to obtain germanenes (Ge-H) or functionalized germanenes (Ge-R , $\text{R} = \text{H}$, or CH_3 or covalent ligands). iii) (Liquid) exfoliation to separate the bundled Ge-R to mono- or few-layer Ge-R from permission of [30]

2.1.1 Synthesis of Functionalized germanane (using topotactical deintercalation)

In the last few years, functionalized germanane was synthesized to further explore electronic properties and the energy storage field. The main feature of the 2D Ge sheet is that it can be chemically functionalized easily, which attracts significant attention to enhance the bandgap and higher density anode material. In addition, the lattice distortions of functionalized germanane are comparatively more stable than the FS Ge sheet. Mainly, functionalized germanane is followed by the topochemical deintercalation of the CaGe_2 film. CaGe_2 was selected because of its Zintl-phase characteristics in high-temperature calcination after MBE fabrication [31]. HCl etched the crystal CaGe_2 film at -40°C , and after washing, the GEH film was observed, as shown in the Figure. 4(a) & (b) [19],[32].

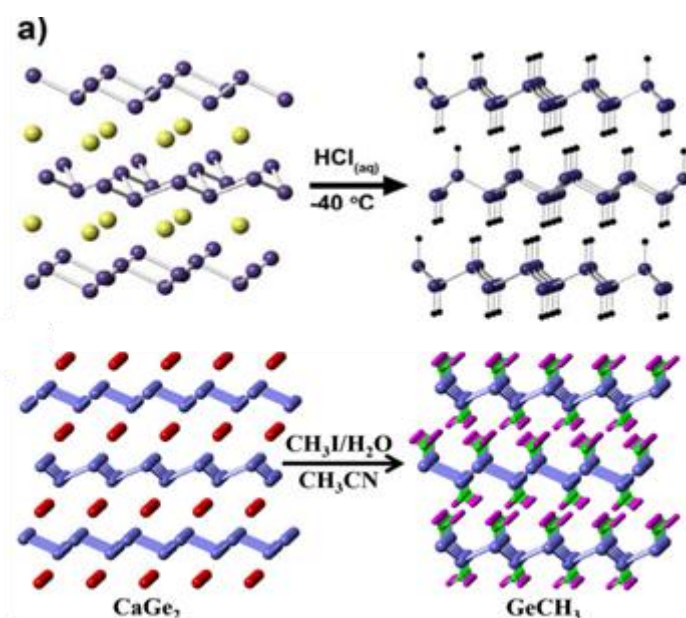


Fig. 4. (a) GeH atomic structure projected by hydrogen termination of the deintercalation by HCl at -40°C with permission of [19]. Green, blue, and red balls are indicated as Ca, Ge, and H, respectively. (b) Methyl termination GeCH_3 nanosheet formation steps using the solvothermal technique with CaGe_2 films from permission of [32].

2.2 Bottom Up

Recently, germanene was constructed on different metals, semimetals, and semiconducting material substrates. Using the metallic substrate, the synthesized germanene becomes a massless Dirac fermion characteristic because of the doping effect and hybridization [11],[12]. On the other hand, the epitaxial growth on semimetal like Sb (111) [33] and semiconductor MoS_2 [2] displayed excellent intrinsic electronic properties of the germanene 2D material.

2.2.1 Epitaxial Growth

I. Au (111) Substrate

High quantum spin hall effect and loss of the massless Dirac fermion character of free-standing germanene were observed on a gold template under ultra-high vacuum conditions by evaporating germanium at $\sim 200^\circ\text{C}$ [34]. The epitaxial growth at the different stages was followed by scanning tunneling microscope (STM) measurements in constant current mode with a tungsten tip.

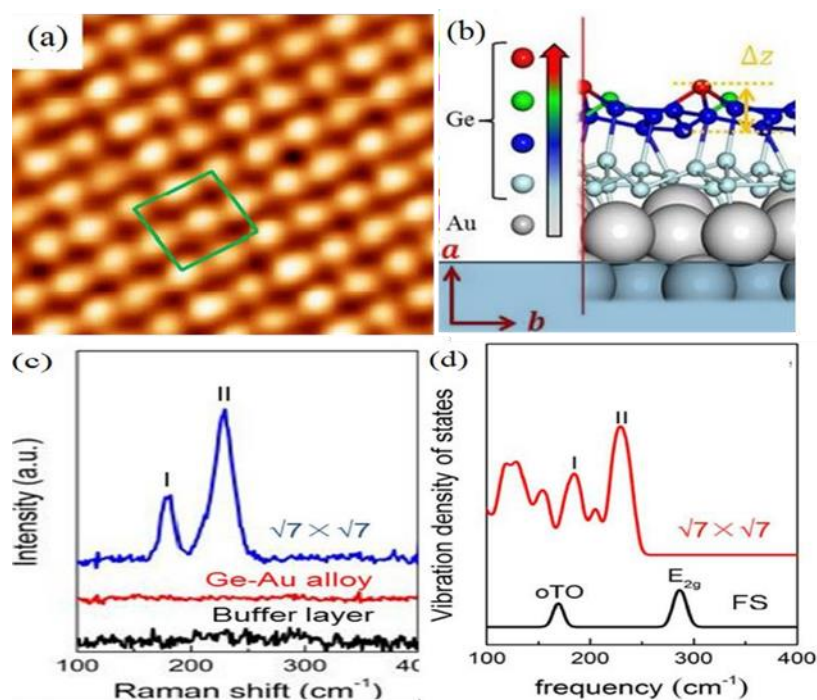


Fig. 5. (a) High resolution STM image of $\sqrt{7}\times\sqrt{7}$ germanene sheet scanned ($4\text{nm} \times 4\text{nm}$, $V_{\text{bias}} = 0.1\text{ V}$, $I = 50\text{ pA}$) voltages (b) Side view of the $\sqrt{7}\times\sqrt{7}$ germanene atomic structure. Different colors are labeled (red, green, dark, and light blue) for the different heights of the Ge atoms buffer layer. The $4\times 2\sqrt{3}$ Au (111) configuration is defined by gray color with permission of (c) Raman spectra of $\sqrt{7}\times\sqrt{7}$ germanene sheet, Ge-Au alloy, and buffer layer. (d) The vibration density of state was calculated by density functional theory (DFT) for FS monolayer germanene and $\sqrt{7}\times\sqrt{7}$ germanene sheet. With permission of [35].

As shown in Fig.5, the honeycomb lattice structure is observed by the STM image for specific voltages and the different buckled heights of the Ge atom layer. The height difference of the upper layer (dark blue and red), Δz , is almost two times that of the free-standing (FS) germanene, which indicates the stable interaction between the Au (111) substrate with adjacent Ge layers and other Ge nanosheets as well [35]. Moreover, the first layer of germanium-gold alloy (buffer layer) exhibits no Raman peak, and FS germanene shows two signals at 179 cm^{-1} and 228 cm^{-1} . These signals significantly correlate with the vibrational modes of out-of-plane transverse optical (oTO) and E_{2g} mode [36]. The Raman shift of the E_{2g} mode of FS germanene occurs for tensile strength and interacts with the carrier of the honeycomb lattice that creates a gapless Dirac point [37]. This phenomenon of the E_{2g} differs from the other 2D materials, including graphene and transition metal dichalcogenides [38],[39].

II. Sb (111) and MoS₂ substrate

The previous study reconstructed the FS Ge sheet on semimetal (Sb) and semiconductor (MoS₂) by epitaxial growth in an ultra-high vacuum system using the constant current of STM [33],[2]. Gou et al. explored the 1×1 lattice of germanene sheet on a semimetal Sb (111) surface by STM and a low buckled honeycomb arrangement calculated by DFT [40]. Figure 6(a) shows the hexagonal close-packed structure of the FS germanene sheet on the Sb (111) surfaces, and Figure. 6(b) also confirms the step edges along with the crystal orientation of the lattice structure [40].

Most interestingly, the fabrication of the bandgap material with the preexisting defect was observed on the MoS₂ surface [40]. The molecular beam epitaxy (MBE) process reconstructs the FS germanene with an extraordinary electronic property. Figure. 6(c) displays the building block of the transition metal chalcogenide, where the Mo atom is encapsulated with two close-packed S atom layers and produces a Tri-layer structure. These atoms highly interact with solid covalent bonds, and the interaction of MoS₂ with germanene is weak van der Waals forces. In Fig. 6(d), several germanium hexagonal vacancy-shaped islands are exhibited on the MoS₂ surface after the deposition at room temperature.

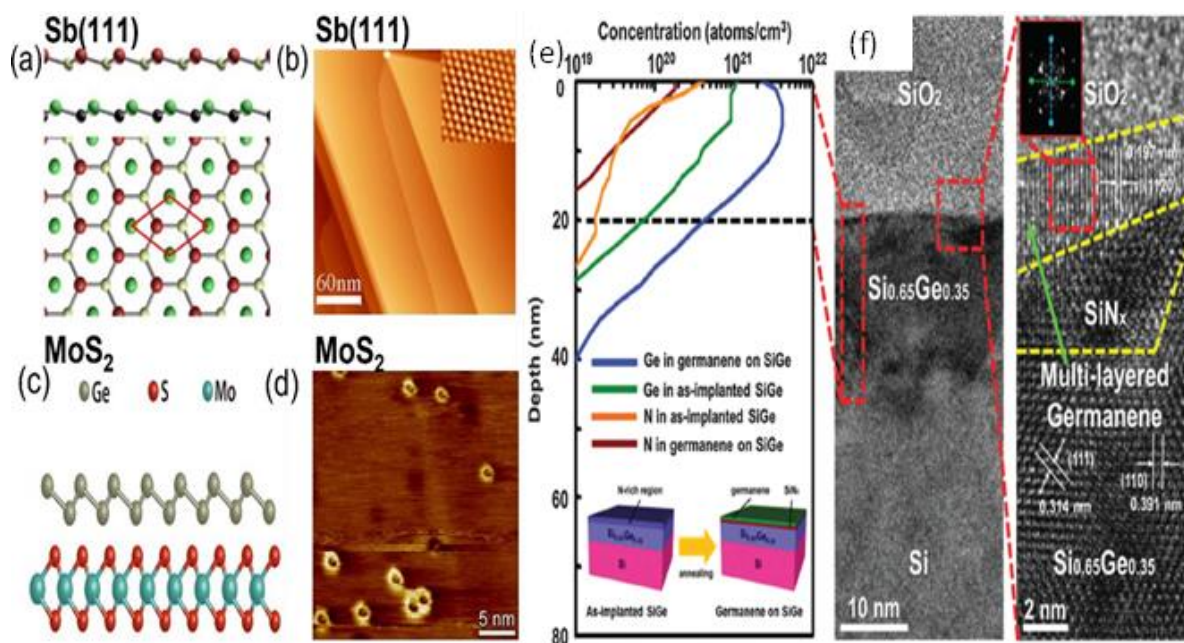


Fig. 6. (a) Side and top view of the FS germanene and Sb (111) surface. Red and yellow balls define the Ge, and red rhombohedra indicate the unit cell of Sb (111) with permission of [40]. (b) STM topological image of the atomic structure on the Sb (111) surface image with permission of [40]. (c) Side view of the atomic structure of transition metal chalcogenides MoS₂ with FS germanene layer [2]. (d) The germanium nucleated with a previous vacancy or defect on the MoS₂ surface from permission of [34]. (e) SIMS depth analysis of Ge and N on SiGe [41]. (f) Higher & lower magnification TEM images of multi-layered germanene from permission of [41].

2.2.2 CVD (Chemical Vapor Deposition)

CVD is one of the prominent and flexible approaches for large-scale multilayer fabrication of germanene 2D material. In most cases, nitrogen plasma and Si wafer as substrates are used for this ultra-high vacuum (UHV) CVD process. Multilayer Si_{0.65}Ge_{0.35} thin film (~2nm) was synthesized using N₂-plasma assisted UHV-CVD process by Tsai et al. and revealed that annealing at high temperatures 5000-8000 C of the fabrication step controls the Ge and N concentration using secondary ion spectrometry (SIMS) depth profile are shown in Fig. 6 (e) [41]. After annealing, N was evaporated, and Ge elements were condensed, forming a crystalline structure of Si_{0.65}Ge_{0.35} layer on Si Substrate [41]. Fig. 6 (f) shows the TEM images of different magnifications of Si_{0.65}Ge_{0.35} thin film on the Si Substrate. Also, the presence of Silicon Nitride (SiN_x) in a higher magnification TEM image confirms the Nitrogen implementation on the substrate during the annealing treatment.

III. PROPERTIES OF GE-2D-BASED NANOMATERIAL

Germanene has been studied and may be considered competitive with other 2D materials in the semiconductor industry for its electrical properties. Considering the first principal calculation using DFT, the relaxation time around the Dirac cone is larger than other 2D materials [5]. On the other hand, it has a low Fermi velocity of about $3.8 \times 10^5 \text{ ms}^{-1}$ in the Dirac cone of the Brillouin zones than graphene $6.3 \times 10^5 \text{ ms}^{-1}$ and silicene $5.1 \times 10^5 \text{ ms}^{-1}$ [42]. Therefore, high ICM ($\sim 6 \times 10^5 \text{ cm}^2 \text{V}^{-1} \text{ s}^{-1}$) was observed in the Boltzmann transport equation with the relaxation time. In addition, the electronic properties depend on the deposition substrate, Fig. 7 (a) and (b). Zhang et al. observed in the density of state (DOS) analysis Figure. 7(c) that the germanene was in 'V' shape around the Fermi level ($\sim 1 \text{ eV}$), and the Fermi energy shifted to 0.3 eV for n-type doping in the system. The QSHE effect on the germanene sheet mainly depends on the bandgap and the atomic structure of the lattice. Liu et al. observed that Ge with a low buckled honeycomb lattice structure displayed as an insulator (bandgap 23.9 meV) and a planar structure exhibited metallic behavior (bandgap 4 eV) [43].

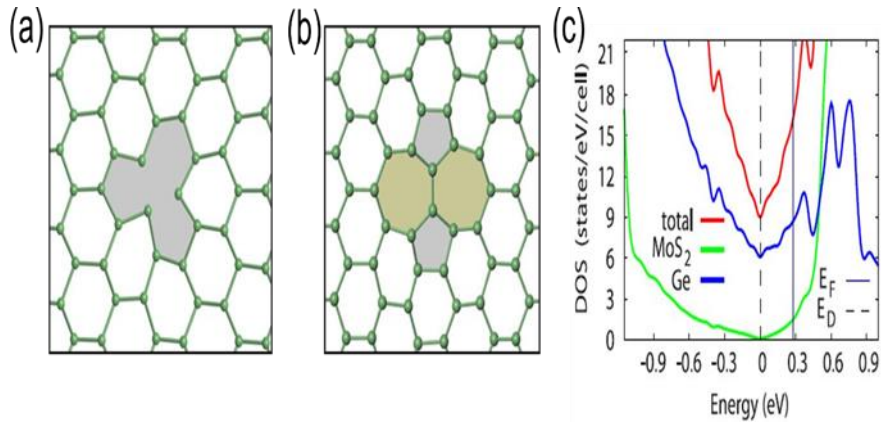


Fig. 7. (a) Vacancy and (b) Stone-Wales defect of germanene sheets after the fabrication on the MoS₂ surface, permission from [17]. (c) DOS calculation of individual and total energy density of germanene on the MoS₂ surface with permission of [02]. Vertical solid and dashed line indicates the Fermi energy and Dirac point.

To further investigate the mechanical properties of FS germanene, the strain was applied in different directions: armchair, zig-zag, chiral (2,1), and (4,1) points, as shown in Fig. 8(a). The stress vs. strain plot, Fig. 8(b), shows the FS germanene sheet's linear elastic formation and the zig-zag direction's highest value. The plane stiffness and intrinsic strength of germanene range from 55.8 N/m to 38.4 N/m and 4.5 N/m to 5.5 N/m in Fig. 8(c). This indicates that the armchair direction will be more difficult to crack or damage than the zig-zag buckled structure for germanene. Ding et al. analyzed the bandgap calculation after applying 15% strain in the armchair and zig-zag direction of the germanene sheet [17]. The lattice symmetry was damaged, the Fermi level changed, and the Dirac point K disappeared and turned into a metallic sheet. Table 1 illustrates the electronic properties of different topotactical deintercalation fabrication techniques of different germanium-based 2D materials based on target application.

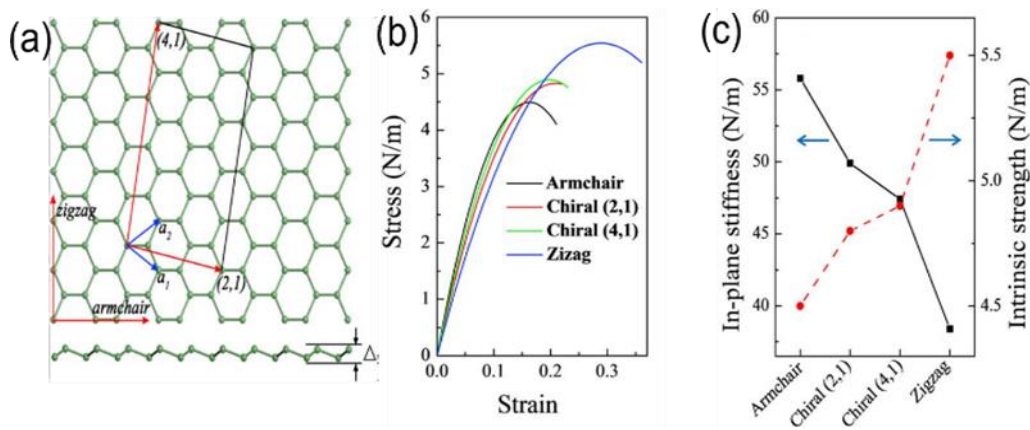


Fig. 8. (a) Different directions (armchair, zig-zag) of FS germanene sheet in atomic structure level with permission of [17]. (b) stress vs. strain curve (c) Stiffness and intrinsic strength of germanene sheet in different directions with permission of [17]

Table 1: Summary of different topotactical deintercalation approaches of Ge-2D nanomaterials, their properties, and applications.

No	Method/Approaches	Properties	Application	Reference
1.	-H termination	Sp ³ hybridized, honeycomb structure, Ge-H nano sheet. Interlayer distance 5.5~5.65Å, thermal stability up to 75 ⁰ C, thermal conductivity of the amorphous ~0.29 Wm ⁻¹ K ⁻¹ , mechanical exfoliated layer size <10 nm, Band Gap 1.65 eV	Photoelectrochemical photodetector, sensor, semiconductor, energy storage.	[18],[44]
2.	-CH ₃ termination	Single step reaction with following S _N 2 or metathesis-like pathway for methyl terminated (Ge-CH ₃ /Ge-Me). Interlayer distance 3.1Å, with greater air and thermal stability up to 250 ⁰ C, Band Gap 1.7 eV, narrower band-edge photoluminescence.	Less defective semiconductor, energy storage, photoluminescence.	[45]
3.	-R (Alkyl) termination	Involves with larger ligands and categorized into complete and partial functionalized germanane. Bond angle 109 ⁰ C due to expansion of α parameter (3.88 Å to 3.96 Å). Alkyl ligands and lower coverage density are exemplified by the photoluminescence properties. Band Gap range (1.84-1.90 eV).	Chemical, Photoelectrochemical photodetector, electrocatalytic, sensor, semiconductor.	[46]
4	Nucleophilic substitution	Different Grignard reagents, including methyl magnesium iodide, phenyl magnesium, and 4-fluorophenylmagnesium bromide, were used to treat CaGe ₂ or Ge ₆ H ₆ . Mainly the F atom in the phenyl atom substituted and germanene acts as an electron sink. Due to fluorescence emission, the distinguishable gap range (2.5 eV-3.0 eV).	Biology, Radiation technology, photoluminescence, photodetector.	[47]
5	Isotopic (-D termination)	Using deuterium chloride (DCl) instead of HCl, -H termination and maintain the charge and chemical properties. The generation of Ge-D only changes the physical properties and increase the Vander Walls gap by ~ 0.3 Å that reduces the band gap 1.53 eV from 1.57 eV.	Optoelectronics, sensor, semiconductor, energy storage.	[48]

IV. APPLICATION OF GE-BASED 2D MATERIAL

The research & development of functionalized 2D germanium nano material continues to unlock new possibilities in materials engineering, paving the way for innovative technologies as illustrated in Fig.9 across electronics, energy storage, sensors, biomedicine, and beyond. The ongoing exploration and refinement of this material promises to redefine the landscape of advanced materials and their applications in the 21st century.

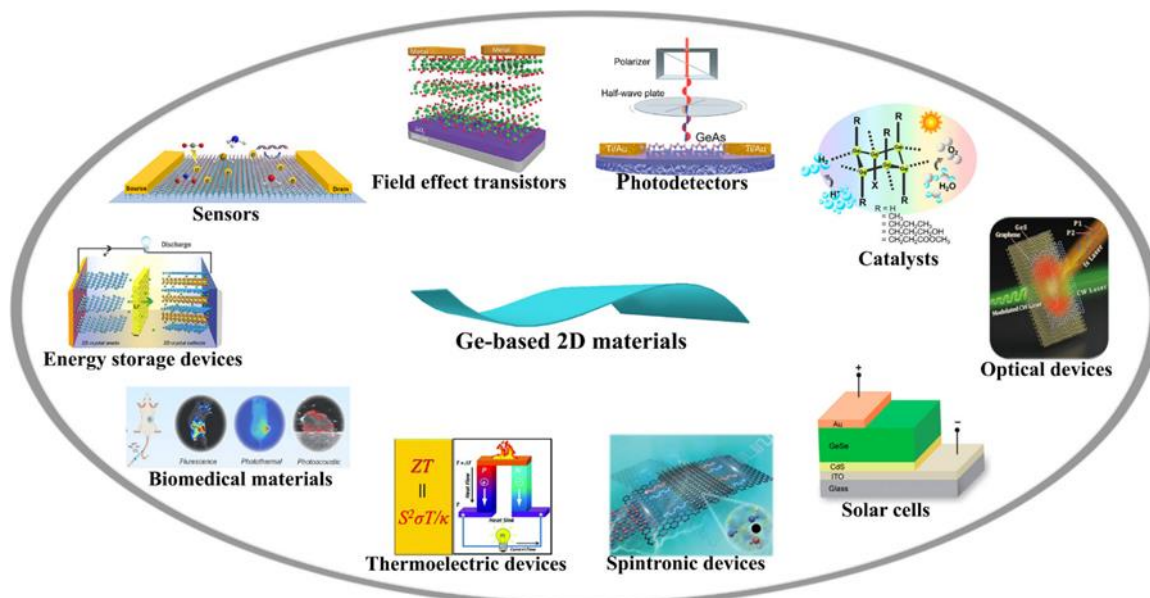


Fig.9: Schematic overview of the application of Ge-based 2D material with permission of [49].

4.1 Energy Storage

Germanium-based 2D material can gain attention as an anode material for architectural design for the Li-ion industry due to its high theoretical capacity (1384 mAh/g for Lithium Germanium), then conventional graphite (372 mAh/g) [50]. Serino, A. C. et al. followed the fabrication method of GeH as an anode material for the Li-ion battery. They claimed a specific capacity of ~ 1100 mAh/g at 0.1C rate at the 1st charge-discharge cycle [50]. A few years back, methyl-terminated germanane (GeCH_3) was fabricated as a high-density anode material by liquid-phase exfoliation to increase layer spacing and better cycle stability of Li-ion batteries [51]. Zhao, F. et al. observed an impressive electrochemical storage capacity (~ 1058 mAh/g after 100 cycles at 0.2C rate), adding reduced graphene oxide (rGO) with GeCH_3 nanocomposite [51].

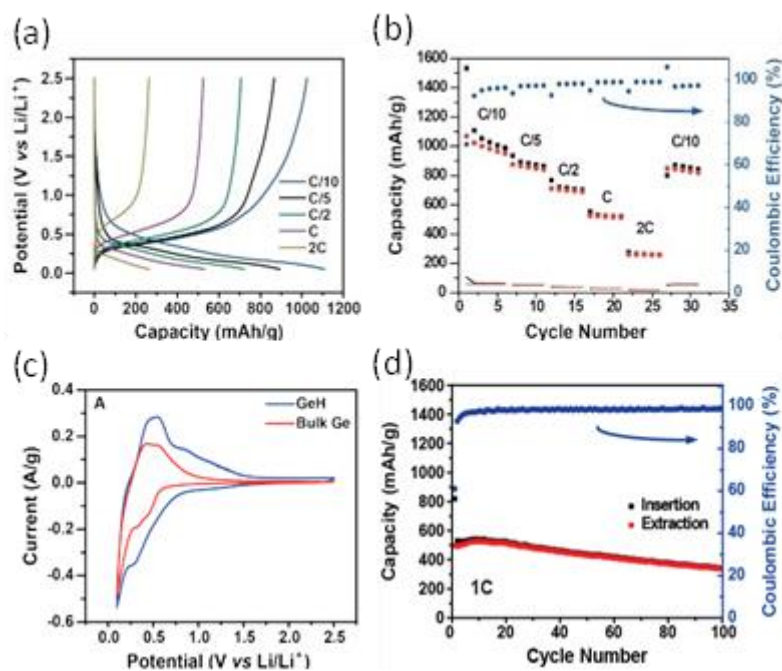


Fig. 10. (a) Charge-discharge profile at different current densities, (b) rate performance with coulombic efficiency, (c) cyclic voltammograms, (d) long-term cyclic performance of functionalized germanane (GeH) as an anode from permission of [50].

In Fig. 10(a), the discharge capacity of GeH anode material shows about 1120 mAh/g at a C/10 rate, which indicates a comparatively higher capacity than conventional graphite. Moreover, the rate performance of the anode material and high coulombic efficiency Fig.10(b) confirms the prospect of this 2D material in the energy conversion field. The CV profile helps to better understand the lithium intercalation and deintercalation from the anode structure. The broad peak observed from 0.4V to 0.6V in Fig. 10(c) indicates the structure's delithiation. Different formation Ge_xL_y phases have been created in different electrochemical potential stages for the lithiation and delithiation of the anode material [50]. Besides, the degradation or capacity fading analysis is shown in Figure. 10(d) indicates cyclic stability after the 100th cycle at 1C rate.

4.2 Biomedical

In recent years, germanene and functionalized germanene 2D materials exhibit significant attraction in biomedical applications owing to their direct and indirect narrow band gap to serve as near-infrared (NIR), photothermal agents (PTA) with high photothermal conversion efficiency (PTCE) [52]. -H termination of germanene 2D material showed a much wider direct bandgap of 1.65 eV (as shown in Fig. 11a.) is a so-called zero band gap material which leads to use in photodynamic therapy (PDT) for various diseases, including wet age-related macular degeneration psoriasis, atherosclerosis, viral infections, neurodegenerative diseases and cancer [53]. Different Reactive Oxygen Species (ROS) generation or transformation can be regulated by optimized PDT therapeutic effect [54], [55]. Germanium 2D nanosheets with phosphorus (GeP) induced a direct bandgap to serve as pH-responsive, heat-stimulative, and sustained-drug-release performance as a chemo photothermal synergistic cancer therapy platform and show remarkable tumor ablation ability [52]. Fig. 11 b. demonstrates the effectiveness of H-germanene used as a potential photosensitizer for PDT of the cell apoptosis of the mouse breast cancer cell line 4T1 and human lung microvascular endothelial cells (HMEVC). Ge et al. investigated the anticancer efficacy of -H germanene on 4T1 BALB/c mice and differentiated the irradiation treatment in four groups (control, H-germanene only, irradiation only, and H-germanene+irradiation groups), which are shown in Fig. 11c & d. The tumor volume was suppressed significantly after the H-germanene+irradiation treatment and increased therapeutic effectiveness. Analogously, germanene quantum dots (GeQDs) are used in the field of photonic cancer nanomedicine due to extraordinary photothermal efficiency (higher than graphene and black phosphorus quantum dots) [55]. To compare different photothermal conversion therapies, Ouyang et al. discovered that polyethylene glycol (PEG@GeQDs) performed superior stability and excellent biocompatibility than conventional control, near-infrared (NIR) treatment [56]. Fig. 11e & f show the mouse tumor volume reduction using different laser treatments.

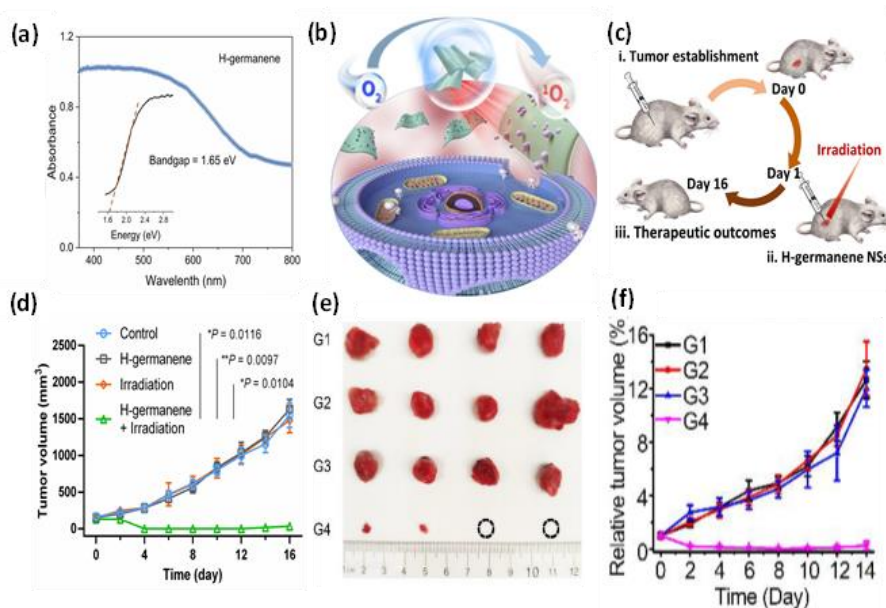


Fig. 11 (a) Structural regulation analysis (UV-vis diffuse reflectance spectra and tauc plots) of H-germanene nanosheet, permission from [53]. Schematic diagram of (b) cell apoptosis induced by PDT & (c) different laser irradiation treatment of anticancer activity, permission from [53]. (d) Tumor volume analysis using different H-germanene groups. Data are presented as means \pm SD (n=5). One-way ANOVA with Tukey's post-hoc test. * $P < 0.05$, ** $P < 0.01$, *** $P < 0.001$ and **** $P < 0.0001$ [56]. (e) Digital images of mouse tumors after different treatments & (f) Relative tumor volumes of mice in different groups where (G1: Control; G2: NIR; G3: PEG@GeQDs; G4: PEG@GeQDs + NIR with permission of [56].

4.3 Others

The functionalized germanene has significant applications in catalysis, optoelectronics, and the luminescence field. Liu et al. reported that GeH exhibits high photo reactivity during the photocatalytic reaction [20]. From our previous study, the bandgap of FS germanene on semiconductor material MoS₂ can be transformed up to 1.8 V, while exfoliated single-layer sheet and high carrier mobility are strong photoluminescence optoelectronic properties. Similarly, Ge also exhibits new structural formation when it is transformed into a 2D format due to the exfoliation of single-layer van der Waals material. Importantly, synthesized GeH and GeCH₃ nanolayers 1-600 nm with a surface area of 1cm² also contain optical properties and characteristics [34]. Therefore, functionalized Ge provides significant insight into future optoelectronic applications.

V. CONCLUSION

This summary illustrates an overview of the promising current research and study on germanium based 2D material synthesis, properties, and applications. The high carrier mobility, QSHE of germanene, and large bandgap properties of germanene motivate further research and analysis in the semiconductor, optoelectronic, and energy storage (Li-metal and Li-ion) conversion sectors. Therefore, understanding the different fabrication techniques is very important it provides valuable insight for the commercialization of germanene. So far, the MBE synthesis method produces high-purity germanene on a low production scale. The key challenge of the functionalized germanene fabrication method is the large production quantity at low temperature. There might be a possibility of an unexpected impurity Ge-Cl bond as a final product that will minimize the photoluminescence property of the 2D material. Therefore, a standard optimized synthesis process should be developed to ensure high-quality germanene and functionalized germanene sheet formation. Also, the characterization technique can be further improved to be utilized in the next generation of electronic, optoelectronic, and thermoelectric applications.

REFERENCE

- [1] R. R. Nair et al., "Fine Structure Constant Defines Visual Transparency of Graphene," *Science*, vol. 320, no. 5881, pp. 1308–1308, Jun. 2008, doi: 10.1126/science.1156965.
- [2] L. Zhang et al., "Erratum: Structural and Electronic Properties of Germanene on MoS₂ [Phys. Rev. Lett. 116 , 256804 (2016)]," *Phys. Rev. Lett.*, vol. 117, no. 5, p. 059902, Jul. 2016, doi: 10.1103/PhysRevLett.117.059902.
- [3] C. L. Kane and E. J. Mele, "Z₂ Topological Order and the Quantum Spin Hall Effect," *Phys. Rev. Lett.*, vol. 95, no. 14, p. 146802, Sep. 2005, doi: 10.1103/PhysRevLett.95.146802.
- [4] C. L. Kane and E. J. Mele, "Quantum Spin Hall Effect in Graphene," *Phys. Rev. Lett.*, vol. 95, no. 22, p. 226801, Nov. 2005, doi: 10.1103/PhysRevLett.95.226801.
- [5] X.-S. Ye, Z.-G. Shao, H. Zhao, L. Yang, and C.-L. Wang, "Intrinsic carrier mobility of germanene is larger than graphene's: first-principle calculations," *RSC Adv*, vol. 4, no. 41, pp. 21216–21220, 2014, doi: 10.1039/C4RA01802H
- [6] M. Houssa, G. Pourtois, V. V. Afanas'ev, and A. Stesmans, "Electronic properties of two-dimensional hexagonal germanium," *Appl. Phys. Lett.*, vol. 96, no. 8, p. 082111, Feb. 2010, doi: 10.1063/1.3332588.
- [7] Z.-Z. Lin and X. Chen, "Transition-metal-decorated germanene as promising catalyst for removing CO contamination in H₂," *Mater. Des.*, vol. 107, pp. 82–89, Oct. 2016, doi: 10.1016/j.matdes.2016.06.020
- [8] B. Mortazavi, A. Dianat, G. Cuniberti, and T. Rabczuk, "Application of silicene, germanene and stanene for Na or Li ion storage: A theoretical investigation," *Electrochimica Acta*, vol. 213, pp. 865–870, Sep. 2016, doi: 10.1016/j.electacta.2016.08.027
- [9] K. Yang, S. Cahangirov, A. Cantarero, A. Rubio, and R. D'Agosta, "Thermoelectric properties of atomically thin silicene and germanene nanostructures," *Phys. Rev. B*, vol. 89, no. 12, p. 125403, Mar. 2014, doi: 10.1103/PhysRevB.89.125403.
- [10] J. Zhuang et al., "Dirac Signature in Germanene on Semiconducting Substrate," *Adv. Sci.*, vol. 5, no. 7, p. 1800207, Jul. 2018, doi: 10.1002/advs.201800207.
- [11] L. Li et al., "Buckled Germanene Formation on Pt(111)," *Adv. Mater.*, vol. 26, no. 28, pp. 4820–4824, Jul. 2014, doi: 10.1002/adma.201400909.
- [12] M. Derivaz et al., "Continuous Germanene Layer on Al(111)," *Nano Lett.*, vol. 15, no. 4, pp. 2510–2516, Apr. 2015, doi: 10.1021/acs.nanolett.5b00085.
- [13] W. Wang and R. I. G. Uhrberg, "Coexistence of strongly buckled germanene phases on Al(111)," *Beilstein J. Nanotechnol.*, vol. 8, pp. 1946–1951, Sep. 2017, doi: 10.3762/bjnano.8.195.
- [14] Y. Fukaya, I. Matsuda, B. Feng, I. Mochizuki, T. Hyodo, and S. Shamoto, "Asymmetric structure of germanene on an Al(111) surface studied by total-reflection high-energy positron diffraction," *2D Mater.*, vol. 3, no. 3, p. 035019, Sep. 2016, doi: 10.1088/2053-1583/3/3/035019
- [15] Z. Qin et al., "Direct Evidence of Dirac Signature in Bilayer Germanene Islands on Cu(111)," *Adv. Mater.*, vol. 29, no. 13, p. 1606046, Apr. 2017, doi: 10.1002/adma.201606046.
- [16] M. E. Dávila, L. Xian, S. Cahangirov, A. Rubio, and G. Le Lay, "Germanene: a novel two-dimensional germanium allotrope akin to graphene and silicene," *New J. Phys.*, vol. 16, no. 9, p. 095002, Sep. 2014, doi: 10.1088/1367-2630/16/9/095002.
- [17] N. Ding, H. Wang, L. Liu, W. Guo, X. Chen, and C.-M. L. Wu, "Effects of mechanical strain on the performance of germanene sheets: Strength, failure behavior, and electronic structure," *J. Phys. Chem. Solids*, vol. 113, pp. 201–209, Feb. 2018, doi: 10.1016/j.jpcs.2017.10.015.
- [18] G. Vogg, M. S. Brandt, and M. Stutzmann, "Polygermyne—A Prototype System for Layered Germanium Polymers," *Adv. Mater.*, vol. 12, no. 17, pp. 1278–1281, Sep. 2000, doi: 10.1002/1521-4095(200009)12:17<1278::AID-ADMA1278>3.0.CO;2-Y.

- [19] E. Bianco, S. Butler, S. Jiang, O. D. Restrepo, W. Windl, and J. E. Goldberger, "Stability and Exfoliation of Germanane: A Germanium Graphane Analogue." *ACS Nano*, vol. 7, no. 5, pp. 4414–4421, May 2013, doi: 10.1021/nn4009406.
- [20] Giousis, T., Potsi, G., Kouloumpis, A., Spyrou, K., Georgantas, Y., Chalmpes, N., ... & Rudolf, P. (2021). Synthesis of 2d germanane (geh): a new, fast, and facile approach. *Angewandte Chemie*, 133(1), 364-369.
- [21] Yuhara, J., Shimazu, H., Ito, K., Ohta, A., Araidai, M., Kurosawa, M., ... & Le Lay, G. (2018). Germanene epitaxial growth by segregation through Ag (111) thin films on Ge (111). *ACS nano*, 12(11), 11632-11637.
- [22] Ledina, M. A., Bui, N., Liang, X., Kim, Y. G., Jung, J., Perdue, B., ... & Stickney, J. L. (2017). Electrochemical formation of germanene: pH 4.5. *Journal of The Electrochemical Society*, 164(7), D469.
- [23] Tsai, H. S., Chen, Y. Z., Medina, H., Su, T. Y., Chou, T. S., Chen, Y. H., ... & Liang, J. H. (2015). Direct formation of large-scale multi-layered germanene on Si substrate. *Physical Chemistry Chemical Physics*, 17(33), 21389-21393.
- [24] Gibaja, C., Rodríguez-San-Miguel, D., Paz, W. S., Torres, I., Salagre, E., Segovia, P., ... & Zamora, F. (2021). Exfoliation of alpha-germanium: a covalent diamond-like structure. *Advanced Materials*, 33(10), 2006826.
- [25] Mazdziaz, M. (2023). Transferability of interatomic potentials for germanene (2D germanium). *Journal of Applied Physics*, 134(18).
- [26] Huey, W. L., & Goldberger, J. E. (2018). Covalent functionalization of two-dimensional group 14 graphane analogues. *Chemical Society Reviews*, 47(16), 6201-6223.
- [27] Wallbaum, H. J. (1944). Über intermetallische Germaniumverbindungen. *Naturwissenschaften*, 32(5), 76-76.
- [28] Vogg, G., Brandt, M. S., & Stutzmann, M. (2000). Polygermyne—A prototype system for layered germanium polymers. *Advanced materials*, 12(17), 1278-1281.
- [29] Jiang, S., Butler, S., Bianco, E., Restrepo, O. D., Windl, W., & Goldberger, J. E. (2014). Improving the stability and optical properties of germanane via one-step covalent methyl-termination. *Nature communications*, 5(1), 3389.
- [30] Ng, S., & Pumera, M. (2023). 2D functionalized germananes: Synthesis and applications. *Advanced Materials*, 35(7), 2207196.
- [31] I. V. Pinchuk, P. M. Odenthal, A. S. Ahmed, W. Amamou, J. E. Goldberger, and R. K. Kawakami, "Epitaxial co-deposition growth of CaGe₂ films by molecular beam epitaxy for large area germanane," *J. Mater. Res.*, vol. 29, no. 3, pp. 410–416, Feb. 2014, doi: 10.1557/jmr.2014.2
- [32] Liu, Z., Wang, Z., Sun, Q., Dai, Y., & Huang, B. (2019). Methyl-terminated germanane GeCH₃ synthesized by solvothermal method with improved photocatalytic properties. *Applied Surface Science*, 467, 881-888.
- [33] J. Lu, X. Zhang, L. Shen, Y. Nie, and G. Xiang, "Two-dimensional Si–Ge monolayers: Stabilities, structures, and electronic properties," *J. Appl. Phys.*, vol. 127, no. 9, p. 094302, Mar. 2020, doi: 10.1063/1.5135079.
- [34] M. E. Dávila and G. Le Lay, "Few layer epitaxial germanene: a novel two-dimensional Dirac material," *Sci. Rep.*, vol. 6, no. 1, p. 20714, Aug. 2016, doi: 10.1038/srep20714.
- [35] J. Zhuang et al., "Cooperative Electron–Phonon Coupling and Buckled Structure in Germanene on Au(111)," *ACS Nano*, vol. 11, no. 4, pp. 3553–3559, Apr. 2017, doi: 10.1021/acsnano.7b00687.
- [36] N. Liu, G. Bo, Y. Liu, X. Xu, Y. Du, and S. X. Dou, "Recent Progress on Germanene and Functionalized Germanene: Preparation, Characterizations, Applications, and Challenges," *Small*, vol. 15, no. 32, p. 1805147, Aug. 2019, doi: 10.1002/sml.201805147
- [37] J. Yan, Y. Zhang, P. Kim, and A. Pinczuk, "Electric Field Effect Tuning of Electron-Phonon Coupling in Graphene," *Phys. Rev. Lett.*, vol. 98, no. 16, p. 166802, Apr. 2007, doi: 10.1103/PhysRevLett.98.166802.
- [38] Y. Wang, C. Cong, C. Qiu, and T. Yu, "Raman Spectroscopy Study of Lattice Vibration and Crystallographic Orientation of Monolayer MoS₂ under Uniaxial Strain," *Small*, vol. 9, no. 17, pp. 2857–2861, Sep. 2013, doi: 10.1002/sml.201202876.
- [39] J. Krustok et al., "Local strain-induced band gap fluctuations and exciton localization in aged WS₂ monolayers," *AIP Adv.*, vol. 7, no. 6, p. 065005, Jun. 2017, doi: 10.1063/1.4985299.
- [40] J. Gou et al., "Strained monolayer germanene with 1 × 1 lattice on Sb(111)," *2D Mater.*, vol. 3, no. 4, p. 045005, Sep. 2016, doi: 10.1088/2053-1583/3/4/045005.
- [41] Tsai, H. S., Chen, Y. Z., Medina, H., Su, T. Y., Chou, T. S., Chen, Y. H., ... & Liang, J. H. (2015). Direct formation of large-scale multi-layered germanene on Si substrate. *Physical Chemistry Chemical Physics*, 17(33), 21389-21393.
- [42] L. C. Lew Yan Voon, E. Sandberg, R. S. Aga, and A. A. Farajian, "Hydrogen compounds of group-IV nanosheets," *Appl. Phys. Lett.*, vol. 97, no. 16, p. 163114, Oct. 2010, doi: 10.1063/1.3495786.
- [43] C.-C. Liu, W. Feng, and Y. Yao, "Quantum Spin Hall Effect in Silicene and Two-Dimensional Germanium," *Phys. Rev. Lett.*, vol. 107, no. 7, p. 076802, Aug. 2011, doi: 10.1103/PhysRevLett.107.076802.
- [44] Roy, P. K., Hartman, T., Šturala, J., Luxa, J., Melle-Franco, M., & Sofer, Z. (2023). Hydrogen-Terminated Two-Dimensional Germanane/Silicene Alloys as Self-Powered Photodetectors and Sensors. *ACS Applied Materials & Interfaces*, 15(21), 25693-25703.
- [45] Jiang, S., Butler, S., Bianco, E., Restrepo, O. D., Windl, W., & Goldberger, J. E. (2014). Improving the stability and optical properties of germanane via one-step covalent methyl-termination. *Nature communications*, 5(1), 3389.
- [46] Ng, S., Šturala, J., Vyskocil, J., Lazar, P., Martincova, J., Plutnar, J., & Pumera, M. (2021). Two-dimensional functionalized germananes as photoelectrocatalysts. *ACS nano*, 15(7), 11681-11693.
- [47] Šturala, J., Luxa, J., Matějková, S., Sofer, Z., & Pumera, M. (2019). Germanane synthesis with simultaneous covalent functionalization: towards highly functionalized fluorescent germananes. *Nanoscale*, 11(41), 19327-19333.
- [48] Kouloumpis, A., Chatzikonstantinou, A. V., Chalmpes, N., Giousis, T., Potsi, G., Katapodis, P., ... & Rudolf, P. (2021). Germanane monolayer films as antibacterial coatings. *ACS Applied Nano Materials*, 4(3), 2333-2338.
- [49] Zhao, F., Feng, Y., & Feng, W. (2022). Germanium-based monoelemental and binary two-dimensional materials: Theoretical and experimental investigations and promising applications. *InfoMat*, 4(11), e12365.
- [50] A. C. Serino et al., "Lithium-Ion Insertion Properties of Solution-Exfoliated Germanane," *ACS Nano*, vol. 11, no. 8, pp. 7995–8001, Aug. 2017, doi: 10.1021/acsnano.7b02589.
- [51] F. Zhao et al., "Few-layer methyl-terminated germanene–graphene nanocomposite with high capacity for stable lithium storage," *Carbon*, vol. 161, pp. 287–298, May 2020, doi: 10.1016/j.carbon.2020.01.072.
- [52] Ren, X., Liu, W., Zhou, H., Wei, J., Mu, C., Wan, Y., ... & Luo, Z. (2022). Biodegradable 2D GeP nanosheets with high photothermal conversion efficiency for multimodal cancer theranostics. *Chemical Engineering Journal*, 431, 134176.
- [53] Ge, M., Guo, H., Zong, M., Chen, Z., Liu, Z., Lin, H., & Shi, J. (2023). Bandgap-engineered germanene nanosheets as an efficient photodynamic agent for cancer therapy. *Angewandte Chemie International Edition*, 62(12), e202215795.
- [54] Ge, J., Lan, M., Zhou, B., Liu, W., Guo, L., Wang, H., ... & Han, X. (2014). A graphene quantum dot photodynamic therapy agent with high singlet oxygen generation. *Nature communications*, 5(1), 4596.
- [55] Idris, N. M., Gnanasammandhan, M. K., Zhang, J., Ho, P. C., Mahendran, R., & Zhang, Y. (2012). In vivo photodynamic therapy using upconversion nanoparticles as remote-controlled nanotransducers. *Nature medicine*, 18(10), 1580-1585.

- [56] Ouyang, J., Feng, C., Ji, X., Li, L., Gutti, H. K., Kim, N. Y., ... & Farokhzad, O. C. (2019). 2D monoelemental germanene quantum dots: synthesis as robust photothermal agents for photonic cancer nanomedicine. *Angewandte Chemie*, 131(38), 13539-13544.